Published in final edited form as:

Biomol NMR Assign. 2023 December ; 17(2): 281–286. doi:10.1007/s12104-023-10156-0.

^{13}C and ^{15}N Resonance Assignments of Alpha Synuclein Fibrils Amplified from Lewy Body Dementia Tissue

Alexander M. Barclay[1,&], **Dhruva D. Dhavale**[2,&], **Collin G. Borcik**[3,4], **Moses H. Milchberg**[3,5], **Paul T. Kotzbauer**[2,*], **Chad M. Rienstra**[3,4,6,*]

[1]Center for Biophysics and Quantitative Biology, University of Illinois at Urbana-Champaign, Urbana, IL 61801, USA

[2]Department of Neurology, Washington University School of Medicine, St. Louis, MO 63110, USA

[3]Department of Biochemistry, University of Wisconsin-Madison, Madison, WI 53706, USA

[4]National Magnetic Resonance Facility at Madison, University of Wisconsin-Madison, Madison, WI 53706, USA

[5]Graduate Program in Biophysics, University of Wisconsin-Madison, Madison, WI 53706, USA

[6]Previous address: Department of Chemistry, University of Illinois at Urbana-Champaign, Urbana, IL 61801 USA

Abstract

Fibrils of the protein α-synuclein (Asyn) are implicated in the pathogenesis of Parkinson Disease, Lewy Body Dementia, and Multiple System Atrophy. Numerous forms of Asyn fibrils have been studied by solid-state NMR and resonance assignments have been reported. Here, we report a new set of ^{13}C, ^{15}N assignments that are unique to fibrils obtained by amplification from postmortem brain tissue of a patient diagnosed with Lewy Body Dementia.

Keywords

α-Synuclein; Fibrils; Lewy Body Dementia; Polymorphism; Parkinson Disease

Biological Context

Alpha-synuclein (Asyn) is a 140-residue protein found in the presynaptic termini of neurons in the brain (Clayton and George 1999). While the exact function of this protein in the brain remains elusive (Lautenschlager, Stephens et al. 2018), the aggregation of

*Correspondence: crienstra@wisc.edu (C.M.R.), kotzbauerp@wustl.edu (P.T.K.).
&These two authors contributed equally to this work.

Author contributions

AMB and DDD made and prepared samples. AMB and CMR collected data. AMB, CGB, MHM and CMR analyzed data, AMB, CGB, MHM, CMR and PTK wrote and prepared manuscript. All authors read and approved the final manuscript.

Ethics approval

All experiments comply with the current laws of the United States, the country in which they were performed.

Competing interests

The authors declare no competing interests.

Asyn in the form of fibrils has been a pathological hallmark of Parkinson Disease (PD), Lewy Body Dementia (LBD) and Multiple System Atrophy (MSA), all which can be classified as α-synucleinopathies. Dementia occurs frequently in PD, sometimes beginning at approximately the same time as motor symptoms (Dementia with Lewy bodies or DLB), or up to 20 years after motor symptoms begin (PD with dementia or PDD). The term LBD encompasses the spectrum of clinical presentations classified as DLB and PDD.

Asyn fibrils have been reported to have a range of tertiary and quaternary structures (Tuttle, Comellas et al. 2016, Schweighauser, Shi et al. 2020), contributing to an emerging understanding of the precise relationships of *in vitro* and ex *vivo* conditions. The *in vitro* structures depend on various factors such as mutations (Polymeropoulos, Lavedan et al. 1997, Kruger, Kuhn et al. 1998, Zarranz, Alegre et al. 2004, Comellas, Lemkau et al. 2011, Lemkau, Comellas et al. 2012, Lemkau, Comellas et al. 2013, Khalaf, Fauvet et al. 2014), cytosolic components (Guilarte 2010, Shin and Chung 2012, Kwakye, Paoliello et al. 2015), lipids (Bodner, Dobson et al. 2009, Bodner, Maltsev et al. 2010, Jakubec, Barias et al. 2021, Mahapatra, Mandal et al. 2021), and metals (Uversky, Li et al. 2001). Growing evidence indicates that distinct polymorphs are associated with pathologic Asyn accumulation in α-synucleinopathies, as detailed by previously reported *ex vivo* studies (Schweighauser et al. 2020, Yang et al. 2022) Therefore, structural determination of these fibrils is vital for advancing the understanding of disease etiology, and to aid the development of polymorph-specific clinical diagnostic tools and novel therapeutics.

We isolated insoluble Asyn fibrils from postmortem LBD tissue. Then, to analyze LBD fibril structure by SSNMR, we amplified the Asyn fibril seeds using uniform [^{13}C, ^{15}N] labeled wild-type Asyn. Here, we report the ^{13}C and ^{15}N chemical shifts for the amplified Asyn fibrils from an LBD autopsy case. The spectra of these postmortem seeded fibrils exhibit resonances that differ from those of previously reported *in vitro* fibril preparations. These findings demonstrate a different arrangement of β-strands, supporting the hypothesis that fibril structure is directly linked to disease phenotype.

Methods and experiments

Protein expression and purification

Expression of uniform [^{13}C, ^{15}N] labeled wild-type Asyn was carried out in *E. coli* BL21(DE3)/pET28a-AS in modified Studier medium M (Studier 2005). The labeling medium contained 3.3 g/L [^{13}C]glucose, 3 g/L [^{15}N]ammonium chloride, 11 mL/L [^{13}C, ^{15}N]Bioexpress (Cambridge Isotope Laboratories, Inc., Tewksbury, MA), 1 mL/L BME vitamins (Sigma), and 90 μg/mL kanamycin. After a preliminary growth in medium containing natural abundance (NA) isotopes, the cells were transferred to the labeling medium at 37 °C to an OD_{600} of 1.2, at which point the temperature was reduced to 25 °C and protein expression induced with 0.5 mM isopropyl β-D-1-thiogalactopyranoside (IPTG) and grown for 15 h to a final OD_{600} of 4.1 and harvested.

Protein purification was done as described previously (Barclay, Dhavale et al. 2018). Briefly, cells were lysed chemically in the presence of Turbonuclease (Sigma) to digest nucleic acids. Purification began with heat denaturation of the cleared lysate, followed by

ammonium sulfate precipitation (Kloepper, Woods et al. 2006). The resolubilized protein was bound to QFF anion exchange resin (GE Healthcare Life Sciences, Marlborough, MA) and eluted using a linear gradient of 0.2–0.6 M NaCl. Fractions containing Asyn monomer, which eluted at about 0.3 M NaCl, were pooled, concentrated, and run over a 26/60 Sephacryl S-200 HR gel filtration column (GE Healthcare Life Sciences) equilibrated in 50 mM Tris-HCl, 100 mM NaCl, pH 8 buffer. Fractions were pooled, concentrated to ~20 mg/mL Asyn, and dialyzed at 4 °C into 10 mM Tris-HCl pH 7.6, 50 mM NaCl, 1 mM DTT, and stored at a concentration of ~14 mg/mL at −80 °C until use. Yields were 95 mg purified AS protein/L growth medium for the uniform [^{13}C, ^{15}N] labeled monomer.

Preparation of Insoluble fraction seeds from LBD, MSA and control postmortem tissue

The protocol to sequentially extract human postmortem brain tissue was adapted from Appel-Cresswell et al[2]. Briefly, gray matter dissected from tissue was sequentially homogenized in four buffers (3 ml/g wet weight of tissue) using Kimble Chase Konte™ dounce tissue grinders (KT885300-0002). In the first step, 300mg of dissected grey matter tissue was homogenized using 20 strokes of Pestle A in High Salt (HS) buffer (50 mM Tris-HCl pH 7.5, 750 mM NaCl, 5 mM EDTA plus Sigma P2714 Protease Inhibitor (PI) cocktail). The homogenate was centrifuged at 100,000 ×g for 20 min at 4 °C and the pellet was homogenized in the next buffer using 20 strokes of Pestle B. Extractions using Pestle B were performed in HS buffer with 1% Triton X-100 with PI, then HS buffer with 1% Triton X-100 and 1 M sucrose, and with 50 mM Tris-HCl, pH 7.4 buffer. In the final centrifugation, the resulting pellet was resuspended in 50 mM Tris-HCl, pH 7.4 buffer (3 ml/g wet weight of tissue). The aliquots of insoluble fraction were stored at −80 °C until use. Similar extraction protocol was followed for LBD, MSA and control cases.

Amplification of isotopically labelled LBD fibrils from LBD insoluble fraction seeds

We amplified LBD-fibrils from gray matter dissected from the caudate region. We incubated insoluble fraction seeds with an Asyn monomer preparation containing isotopically labeled Asyn monomer supplemented with control fraction. The control fraction preparation was derived from E.Coli transformed with an empty expression vector, and was purified with the same protocol as the natural abundance Asyn monomer (JBC, 2017 V292, Pg9034). Asyn monomer and control fraction was filtered through a 50k MWCO Amicon Ultra centrifugation filter (Millipore, UFC805204) before use, to remove any preformed aggregates.

Insoluble fraction (10 μL) containing 3.3 μg wet wt. of tissue was brought to a final volume of 30 μL by addition of 20 mM Tris-HCl, pH 8.0 plus 100 mM NaCl buffer (fibril buffer) in a 1.7mL microcentrifuge tube. The insoluble fraction was sonicated for 2 min at amplitude 50 in a bath sonicator (Qsonica model Q700) with a cup horn (5.5 inch) attachment at 4 °C. 1.5 μL of 2 % Triton X-100 was added to the sonicated seeds. To this mixture, 50k Amicon ultra filtered isotopically labelled Asyn monomer was added to a final concentration of 2 mg/mL in a final volume of 100 μL. This mixture underwent quiescent incubation at 37 °C for 3 days, completing the 1st round of sonication plus incubation. After the first round, the mixture was sonicated at 1 min at amplitude 50, and then an additional 300 μL of 2 mg/mL Asyn monomer was added. The mixture underwent quiescent incubation at 37 °C for 2 days

(2nd round). Then, sonication for 1 min at amplitude 50 and quiescent incubation for 2 days was repeated for the third round, followed by sonication for 1 min at amplitude 50 and quiescent incubation for 3 days for the 4th round. At the end of 4th round, LBD-amplified fibrils were stored at 4 °C until use.

Further expansion of the LBD-amplified fibrils was performed by centrifuging 60 μL of 4th round LBD-amplified fibrils at 21,000 xg for 15 min at 4 °C. The pellet was resuspended in 100 μL of fibril buffer and sonicated for 1 min at amplitude 50. To this mixture, Asyn monomer was added to a final concentration of 2 mg/mL in a final volume of 400 μL in fibril buffer. This mix was quiescently incubated at 37 °C for 2 days (5th round). At the end of 5th round, samples were centrifuged at 21,000 xg for 15 min at 4 °C and the top 300 μL of spent Asyn monomer was moved to a separate tube. The pellet was resuspended by trituration and sonicated for 1 min at amplitude 50. After sonication, the previously removed 300 μL of 5th round monomer was added back. Next, an additional 2.5 mg/mL of Asyn monomer was added to bring the total volume to 800 μL. This mixture was incubated at 37 °C for 2 days to complete 6th round of incubation. The increased monomer concentration (2.5 mg/mL instead of 2 mg/mL) was calculated based on the average decrease in free Asyn monomer due to its incorporation into amplified fibrils. The 6th round fibrils were stored at 4 °C until use.

Solid-state NMR spectroscopy

Magic-angle spinning (MAS) SSNMR experiments were performed at magnetic field of 11.7 T (500 MHz ^{1}H frequency) or 17.6 T (750 MHz ^{1}H frequency) using Agilent Technologies VNMRS spectrometers. Spinning was controlled with a Varian MAS controller to 11,111 ± 30 Hz or 22,222 ± 15 Hz (11.7 T) and 16,667 ± 15 Hz or 33,333 ± 30 Hz (17.6 T). All experiments were done with a variable-temperature (VT) airflow setting of 0 °C, primarily to keep samples cool from RF and MAS heating, without freezing out molecular motions. The 11.7 T magnet was equipped with a 1.6 mm HCDN T3 probe (Varian), with pulse widths of about 1.8 μs for ^{1}H and ^{13}C, and 3.2 μs for ^{15}N. The 17.6 T magnet was equipped with a HXYZ T3 probe (Varian) tuned to HCN triple resonance mode with pulse widths of about 1.9 μs for ^{1}H, 2.6 μs for ^{13}C, and 3.0 μs for ^{15}N. All experiments utilized ^{1}H-^{13}C or ^{1}H-^{15}N tangent ramped CP (Metz, Wu et al. 1994) and ~100 kHz SPINAL-64 decoupling during evolution and acquisition periods (Fung, Khitrin et al. 2000, Comellas, Lopez et al. 2011). Where applicable, SPECIFIC CP was used for ^{15}N-^{13}Cα and ^{15}N-^{13}C’ transfers (Baldus, Petkova et al. 1998), ^{13}C-^{13}C homonuclear mixing was performed using DARR (Takegoshi, Nakamura et al. 2001). Chemical shifts were externally referenced to the downfield peak of adamantane at 40.48 ppm (Morcombe and Zilm 2003). NUS schedules using biased exponential sampling were prepared using the nus-tool application in NMRbox (Maciejewski, Schuyler et al. 2017). Data conversion and processing was done with NMRPipe (Delaglio, Grzesiek et al. 1995). NUS data was first expanded with the nusExpand.tcl script in NMRPipe, converted, and processed using the built-in SMILE reconstruction function (Ying, Delaglio et al. 2017). Peak picking and chemical shift assignments were performed using NMRFAM-Sparky (Lee, Tonelli et al. 2015).

Extent of assignments and data deposition

Chemical shift assignments were performed for the LBD Asyn fibrils amplified using uniform [^{13}C, ^{15}N] labeling (uCN). Resonance assignments were determined using 2D ^{13}C-^{13}C, 2D ^{15}N-^{13}Cα, 2D ^{15}N-^{13}C', 3D ^{15}N-^{13}Cα-^{13}CX, 3D ^{15}N-^{13}C'-^{13}CX, 3D ^{15}N-^{13}C'-^{13}Cα and 3D ^{13}Cα-^{15}N-^{13}C' data sets following standard procedures (Comellas and Rienstra, 2013; Higman, 2018). The 2D ^{15}N-^{13}C' (Figure 1A) and ^{15}N-^{13}Cα (Figure 1B) spectra serve as structural fingerprints for the fibril, with a focus on the backbone atoms. Critically, these highlight the benefit of adding a ^{15}N dimension to disambiguate shifts, particularly for the Ala and Gly regions, which comprise 30% of the primary sequence between residues 30 and 100, as well as for key core residues like V71, V74, T75 and V77. Overall, there appears to be a predominant defined conformation that likely displays some localized heterogeneity. Figure 2 demonstrates representative strips corresponding to assignments from 3D ^{15}N-^{13}Cα-^{13}CX, 3D ^{15}N-^{13}C'-^{13}CX, and 3D ^{13}Cα-^{15}N-^{13}C' from T72 to A76.

Comparison to previously structurally characterized fibril

We compare the chemical shift assignments of the postmortem seeded LBD fibrils to the extensively studied *in vitro* fibril preparation (PDB: 2N0A). Figure 3 summarizes the differences in the chemical shift values that lead us to the conclusion that the postmortem seeded LBD fibrils presented herein are wholly different than the *in vitro* fibril preparations. This is based chiefly on two observations from extensive assignments of both fibril types. First, due to differences in dynamics or line broadening attributed to multiple confirmations, amino acid sequences that can be unambiguously sequentially assigned within the primary structure of Asyn are different. We discount the possibility of multiple confirmations being present as there is a single set of resonances assignable to each visible peak within the spectrum with no unambiguous peaks assignable to consecutive stretches from the 2D and 3D datasets. Secondly, unambiguous chemical shifts that are common between *in vitro* and postmortem seeded fibrils display significant chemical shift differences, with an average of ~1.9 ppm, when scaled with respect to ^{15}N and ^{13}C chemical shift values.

Acknowledgments

Support for this work was provided by: grants from the Michael J. Fox Foundation; NIH grants NS110436, NS097799, and NS075321 from the National Institute of Neurological Disorders and Stroke and National Institute on Aging and P41GM136463 from the National Institute of General Medical Sciences. CDS was supported by the Intramural Research Programs of NIDDK and NHLBI at the National Institutes of Health. We thank Deborah Berthold for assistance with production of isotopically-labeled recombinant Asyn protein.

Funding

Support for this work was provided by: grants from the Michael J. Fox Foundation; NIH grants NS110436, NS097799, and NS075321 from the National Institute of Neurological Disorders and Stroke and National Institute on Aging and P41GM136463 (CMR) from the National Institute of General Medical Sciences.

Data availability

Resonance assignments are available through the Biological Magnetic Resonance Data Bank (http://bmrb.io), Accession Number 51678.

References

Baldus M, Petkova AT, Herzfeld J and Griffin RG (1998). "Cross polarization in the tilted frame: assignment and spectral simplification in heteronuclear spin systems." Molecular Physics 95(6): 1197–1207.

Barclay AM, Dhavale DD, Courtney JM, Kotzbauer PT and Rienstra CM (2018). "Resonance assignments of an alpha-synuclein fibril prepared in Tris buffer at moderate ionic strength." Biomol NMR Assign 12(1): 195–199. [PubMed: 29476328]

Bodner CR, Dobson CM and Bax A (2009). "Multiple tight phospholipid-binding modes of alpha-synuclein revealed by solution NMR spectroscopy." J Mol Biol 390(4): 775–790. [PubMed: 19481095]

Bodner CR, Maltsev AS, Dobson CM and Bax A (2010). "Differential phospholipid binding of alpha-synuclein variants implicated in Parkinson's disease revealed by solution NMR spectroscopy." Biochemistry 49(5): 862–871. [PubMed: 20041693]

Clayton DF and George JM (1999). "Synucleins in synaptic plasticity and neurodegenerative disorders." J Neurosci Res 58(1): 120–129. [PubMed: 10491577]

Comellas G, Lemkau LR, Nieuwkoop AJ, Kloepper KD, Ladror DT, Ebisu R, Woods WS, Lipton AS, George JM and Rienstra CM (2011). "Structured regions of alpha-synuclein fibrils include the early-onset Parkinson's disease mutation sites." J Mol Biol 411(4): 881–895. [PubMed: 21718702]

Comellas G, Lopez JJ, Nieuwkoop AJ, Lemkau LR and Rienstra CM (2011). "Straightforward, effective calibration of SPINAL-64 decoupling results in the enhancement of sensitivity and resolution of biomolecular solid-state NMR." J Magn Reson 209(2): 131–135. [PubMed: 21296014]

Delaglio F, Grzesiek S, Vuister GW, Zhu G, Pfeifer J and Bax A (1995). "Nmrpipe - a Multidimensional Spectral Processing System Based on Unix Pipes." Journal of Biomolecular Nmr 6(3): 277–293. [PubMed: 8520220]

Fung BM, Khitrin AK and Ermolaev K (2000). "An improved broadband decoupling sequence for liquid crystals and solids." J Magn Reson 142(1): 97–101. [PubMed: 10617439]

Guilarte TR (2010). "Manganese and Parkinson's disease: a critical review and new findings." Environ Health Perspect 118(8): 1071–1080. [PubMed: 20403794]

Jakubec M, Barias E, Furse S, Govasli ML, George V, Turcu D, Iashchishyn IA, Morozova-Roche LA and Halskau O (2021). "Cholesterol-containing lipid nanodiscs promote an alpha-synuclein binding mode that accelerates oligomerization." FEBS J 288(6): 1887–1905. [PubMed: 32892498]

Khalaf O, Fauvet B, Oueslati A, Dikiy I, Mahul-Mellier AL, Ruggeri FS, Mbefo MK, Vercruysse F, Dietler G, Lee SJ, Eliezer D and Lashuel HA (2014). "The H50Q mutation enhances alpha-synuclein aggregation, secretion, and toxicity." J Biol Chem 289(32): 21856–21876. [PubMed: 24936070]

Kloepper KD, Woods WS, Winter KA, George JM and Rienstra CM (2006). "Preparation of alpha-synuclein fibrils for solid-state NMR: expression, purification, and incubation of wild-type and mutant forms." Protein Expr Purif 48(1): 112–117. [PubMed: 16564705]

Kruger R, Kuhn W, Muller T, Woitalla D, Graeber M, Kosel S, Przuntek H, Epplen JT, Schols L and Riess O (1998). "Ala30Pro mutation in the gene encoding alpha-synuclein in Parkinson's disease." Nat Genet 18(2): 106–108. [PubMed: 9462735]

Kwakye GF, Paoliello MM, Mukhopadhyay S, Bowman AB and Aschner M (2015). "Manganese-Induced Parkinsonism and Parkinson's Disease: Shared and Distinguishable Features." Int J Environ Res Public Health 12(7): 7519–7540. [PubMed: 26154659]

Lautenschlager J, Stephens AD, Fusco G, Strohl F, Curry N, Zacharopoulou M, Michel CH, Laine R, Nespovitaya N, Fantham M, Pinotsi D, Zago W, Fraser P, Tandon A, St George-Hyslop P, Rees E, Phillips JJ, De Simone A, Kaminski CF and Schierle GSK (2018). "C-terminal calcium binding of alpha-synuclein modulates synaptic vesicle interaction." Nat Commun 9(1): 712. [PubMed: 29459792]

Lee W, Tonelli M and Markley JL (2015). "NMRFAM-SPARKY: enhanced software for biomolecular NMR spectroscopy." Bioinformatics 31(8): 1325–1327. [PubMed: 25505092]

Lemkau LR, Comellas G, Kloepper KD, Woods WS, George JM and Rienstra CM (2012). "Mutant protein A30P alpha-synuclein adopts wild-type fibril structure, despite slower fibrillation kinetics." J Biol Chem 287(14): 11526–11532. [PubMed: 22334684]

Lemkau LR, Comellas G, Lee SW, Rikardsen LK, Woods WS, George JM and Rienstra CM (2013). "Site-specific perturbations of alpha-synuclein fibril structure by the Parkinson's disease associated mutations A53T and E46K." PLoS One 8(3): e49750. [PubMed: 23505409]

Maciejewski MW, Schuyler AD, Gryk MR, Moraru II, Romero PR, Ulrich EL, Eghbalnia HR, Livny M, Delaglio F and Hoch JC (2017). "NMRbox: A Resource for Biomolecular NMR Computation." Biophysical Journal 112(8): 1529–1534. [PubMed: 28445744]

Mahapatra A, Mandal N and Chattopadhyay K (2021). "Cholesterol in Synaptic Vesicle Membranes Regulates the Vesicle-Binding, Function, and Aggregation of alpha-Synuclein." J Phys Chem B 125(40): 11099–11111. [PubMed: 34473498]

Metz G, Wu XL and Smith SO (1994). "Ramped-Amplitude Cross-Polarization in Magic-Angle-Spinning Nmr." Journal of Magnetic Resonance Series A 110(2): 219–227.

Morcombe CR and Zilm KW (2003). "Chemical shift referencing in MAS solid state NMR." Journal of Magnetic Resonance 162(2): 479–486. [PubMed: 12810033]

Polymeropoulos MH, Lavedan C, Leroy E, Ide SE, Dehejia A, Dutra A, Pike B, Root H, Rubenstein J, Boyer R, Stenroos ES, Chandrasekharappa S, Athanassiadou A, Papapetropoulos T, Johnson WG, Lazzarini AM, Duvoisin RC, Di Iorio G, Golbe LI and Nussbaum RL (1997). "Mutation in the alpha-synuclein gene identified in families with Parkinson's disease." Science 276(5321): 2045–2047. [PubMed: 9197268]

Schweighauser M, Shi Y, Tarutani A, Kametani F, Murzin AG, Ghetti B, Matsubara T, Tomita T, Ando T, Hasegawa K, Murayama S, Yoshida M, Hasegawa M, Scheres SHW and Goedert M (2020). "Structures of alpha-synuclein filaments from multiple system atrophy." Nature 585(7825): 464–469. [PubMed: 32461689]

Shin HW and Chung SJ (2012). "Drug-induced parkinsonism." J Clin Neurol 8(1): 15–21. [PubMed: 22523509]

Studier FW (2005). "Protein production by auto-induction in high-density shaking cultures." Protein Expression and Purification 41(1): 207–234. [PubMed: 15915565]

Takegoshi K, Nakamura S and Terao T (2001). "C-13-H-1 dipolar-assisted rotational resonance in magic-angle spinning NMR." Chemical Physics Letters 344(5-6): 631–637.

Tuttle MD, Comellas G, Nieuwkoop AJ, Covell DJ, Berthold DA, Kloepper KD, Courtney JM, Kim JK, Barclay AM, Kendall A, Wan W, Stubbs G, Schwieters CD, Lee VM, George JM and Rienstra CM (2016). "Solid-state NMR structure of a pathogenic fibril of full-length human alpha-synuclein." Nat Struct Mol Biol 23(5): 409–415. [PubMed: 27018801]

Uversky VN, Li J and Fink AL (2001). "Metal-triggered structural transformations, aggregation, and fibrillation of human alpha-synuclein. A possible molecular NK between Parkinson's disease and heavy metal exposure." J Biol Chem 276(47): 44284–44296. [PubMed: 11553618]

Yang Y, Shi Y, Schweighauser M, Zhang X, Kotecha A, Murzin AG, et al. (2020). "Structures of alpha-synuclein filaments from human brains with Lewy pathology." Nature 7933(610): 791–795.

Ying J, Delaglio F, Torchia DA and Bax A (2017). "Sparse multidimensional iterative lineshape-enhanced (SMILE) reconstruction of both non-uniformly sampled and conventional NMR data." J Biomol NMR 68(2): 101–118. [PubMed: 27866371]

Zarranz JJ, Alegre J, Gomez-Esteban JC, Lezcano E, Ros R, Ampuero I, Vidal L, Hoenicka J, Rodriguez O, Atares B, Llorens V, Gomez Tortosa E, del Ser T, Munoz DG and de Yebenes JG (2004). "The new mutation, E46K, of alpha-synuclein causes Parkinson and Lewy body dementia." Ann Neurol 55(2): 164–173. [PubMed: 14755719]

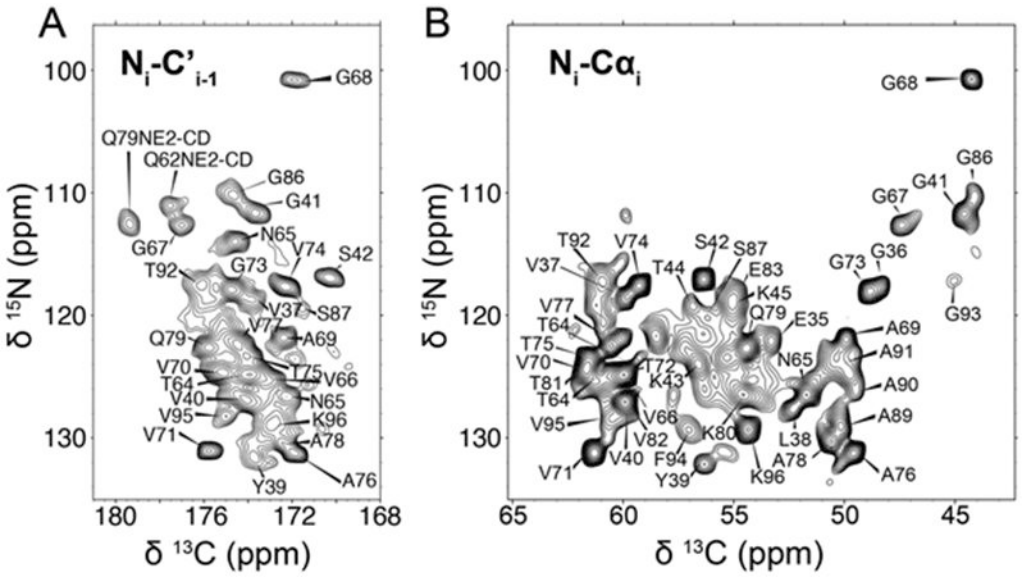

Figure 1:

Backbone chemical shift assignments demarked on a ^{15}N-^{13}C' (A) and a ^{15}N-^{13}Cα (B) spectra.

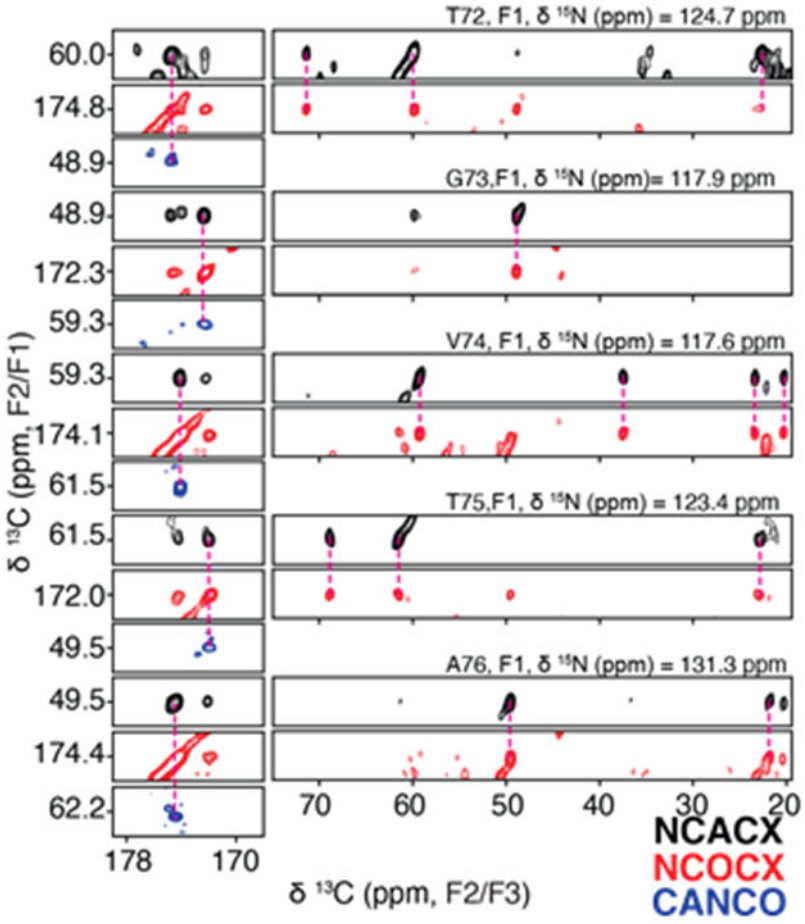

Figure 2:

Example backbone assignment strip from T72 to A76 demonstrating connectivity and sidechain assignments from a 3D ^{15}N-^{13}Cα-^{13}CX correlation (black), a 3D ^{15}N-^{13}C'-^{13}CX correlation (red), and a 3D ^{13}Cα-^{15}N-^{13}C'correlation (blue).

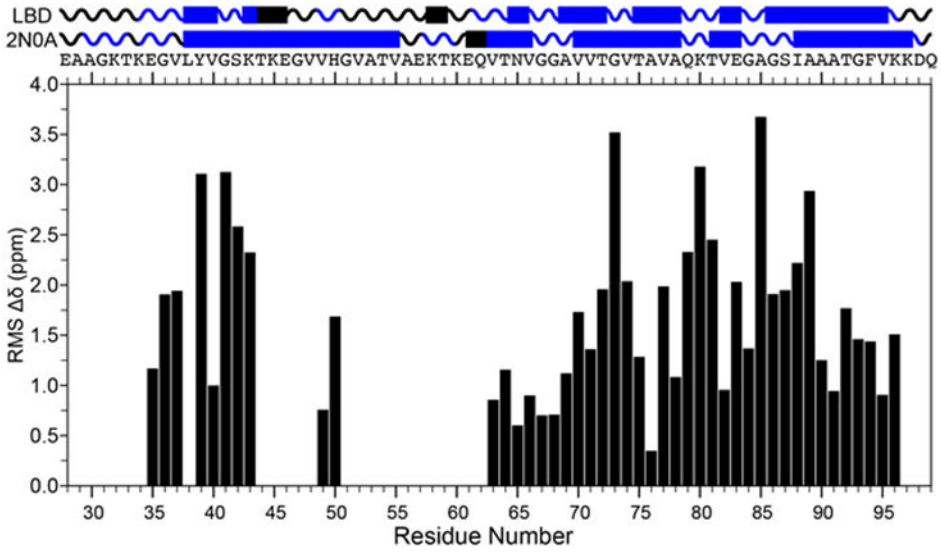

Figure 3:

Secondary structure and chemical shift comparison between postmortem seeded LBD and PDB ID: 2N0A. Top: Predicted secondary structure of the LBD case versus the structure of the *in vitro* fibril form from residues 28 to 99. The primary structure is labeled under the secondary structure for reference. Bottom: Plot of the residue specific chemical shift RMS differences of the LBD postmortem seeded case to the *in vitro* 2N0A case. RMS Δδ was calculated as $\Delta\delta = \{\sum_i [(\Delta\delta_{Ci})^2 + (0.4 \times \Delta\delta_N)^2] / n\}^{1/2}$, where i refers to α, β, γ, δ, and ε and n is the number of assignments used to perform the calculation.